Forced Oscillations near the Critical Latitude for Diurnal-Inertial Resonance

J. H. SIMPSON, P. HYDER, AND T. P. RIPPETH

School of Ocean Sciences, University of Wales, Bangor, Menai Bridge, Anglesey, United Kingdom

I. M. LUCAS

Fugro Geos Ltd. Swindon, United Kingdom

(Manuscript received 28 August 2000, in final form 12 June 2001)

ABSTRACT

Oscillations at, or close to, the inertial frequency are widely observed in shelf seas where frictional damping is weak. In the vicinity of latitudes 30°N and S, such motions may become significantly enhanced by a resonance in which the local inertial frequency coincides with that of diurnal forcing. Under these conditions, regular daily variations in wind stress tend to produce large anticyclonic motions that may extend throughout the water column as shown in the analytical theory of Craig. Here the authors examine new observations from a location close to the critical latitude on the Namibian shelf in the Southern Hemisphere. The measurements cover almost the full depth (175 m) of the water column by using upward and downward looking ADCPs suspended in midwater. The observed flow involves a steady drift to the north (maximum ~11 cm s^{-1} at 40 m) but the kinetic energy budget is dominated by anticyclonic circular motions with speeds in the surface layers exceeding 40 cm s^{-1} at times. Comparably energetic motions (speed >35 cm s^{-1}) were found in the lower layers of the stratified water column where, below 70 m, there was a consistent phase shift, relative to the near-surface motion, of ~180°. During the observation period, the winds at the nearest land station, 130 km distant, exhibited significant diurnal variation with a stress magnitude of up to 0.1 Pa and almost equal, and in-phase, components of coast-normal and coast-parallel wind stress. The principal features of the observations are interpreted in terms of an analytical model of two uncoupled layers in which the bottom layer is forced by through the coast-normal pressure gradient set up by the oscillatory wind stress. This pressure gradient is of comparable magnitude, but opposite in phase, to the surface forcing and this accounts for the relatively energetic phase-shifted motions in the lower layers. In areas of low tidal energy close to the critical latitude, diurnal oscillations of the kind observed here should be considered as an important candidate source for vertical mixing.

1. Introduction

Anticyclonic circular motions of the surface layers of the ocean have long been recognized as energetic features of the circulation since observations by Helland-Hansen and Ekman (1931) in the Atlantic and Gustafson and Kullenberg (1933) in the Baltic. They are widely reported in the modern literature from a great variety of locations (e.g., Webster 1968; Pollard 1980; Millot and Crepon 1981; Webster 1986; Schahinger 1988; Poulain 1990; Salat et al. 1992) and seem to be an almost ubiquitous feature of oceanic motion except where frictional damping is high. Most frequently these motions are at, or close to, the local inertial frequency f when they involve a dynamic balance between the geostrophic and radial accelerations. Such ''inertial oscillations'' occur most obviously in response to changes in the wind stress vector (Pollard and Millard 1970) but may also form the transient response in other dynamical adjustments. They are the ''free'' motions of water particles in response to impulsive injections of momentum and, where the frictional damping is weak, may persist for many oscillatory cycles (e.g., Poulain 1990). The motion is generally strongest in the surface layers but some energy propagates down through the water column as inertial waves inducing significant inertial currents in deep water. Marked changes in amplitude and phase at the bottom of the surface mixed layer involve strong vertical shears, which may be responsible for promoting vertical mixing across the pycnocline (Pollard et al. 1973).

An alternative form of circular motion is the response induced by periodic forcing at a particular frequency. The theory of the response to this kind of regular forcing, after the decay of transients, has been explored in two illuminating papers by Craig (1989a,b). In addition to the well-known example of motions driven by the semidiurnal and diurnal tides (Battisti and Clarke 1982), there is also the possibility of forcing by a diurnal variation in wind stress. A

Corresponding author address: Dr. John H. Simpson, School of Ocean Sciences, University of Wales, Bangor, Menai Bridge, Anglesey LL59 5EY, United Kingdom.
E-mail: j.h.simpson@bangor.ac.uk

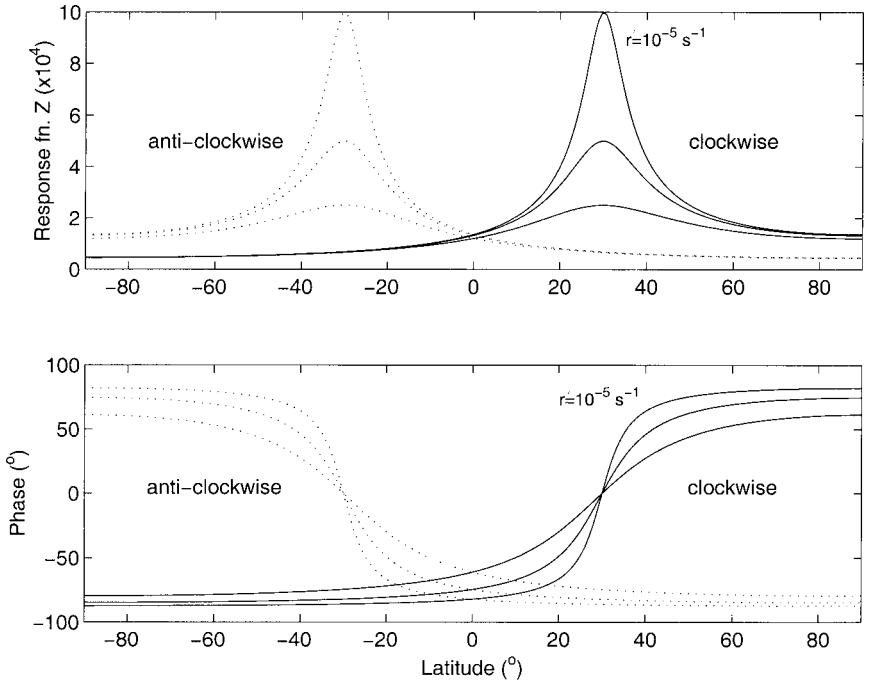

FIG. 1. Variation of the response function $Z = W/A$ with latitude for a simple slab model of forced oscillations with $r' = 10^{-5}$, 2×10^{-5}, 4×10^{-5} s^{-1}. The amplitude (a) and phase (b) are shown for clockwise (solid line) and anticlockwise (dotted line).

pattern of onshore sea breeze during the day followed by offshore winds at night is a characteristic feature of many coastal boundary regions. The wind speed associated with sea breezes is typically 2–5 m s^{-1} but may exceed 10 m s^{-1} in some cases (Pattiaratchi et al. 1997) and extend more than 100 km offshore from the coast (Simpson 1994). Current oscillations driven by the diurnal wind stress are less extensively reported in the literature than inertial motions but clear examples are given in Rosenfeld (1988), Chen et al. (1996), and DiMarco et al. (2000).

The focus of this paper is on the situation where the period of free oscillations f is close to the period of the diurnal forcing by wind stress and a near-resonant response occurs. The essential mechanism and latitudinal variation is illustrated by a simple slab model for a water column of depth H in which the velocity is assumed to be vertically uniform and the motion driven by an oscillating wind stress τ_s with no horizontal pressure gradients. If the motion is damped by a linearized friction $(-ru, -rv)$ the dynamical equations for the complex velocity $w = u + iv$ can be written:

$$\frac{\partial w}{\partial t} + ifw = \frac{-rw + \tau_s}{\rho H}. \qquad (1)$$

The complex amplitudes for clockwise (W_-) and anticlockwise (W_+) forcing at frequency ω are just:

$$W_- = \frac{A_-}{i(f - \omega) + r'}; \qquad W_+ = \frac{A_+}{i(f + \omega) + r'}, \qquad (2)$$

where $\tau_s/(\rho H) = A_\pm e^{\pm i\omega t}$ and $r' = r/(\rho H)$. The response (Fig. 1) is resonant ($W \to A/r'$) for the clockwise case at 30°N where $f = \omega$ and for the anticlockwise case at 30°S ($f = -\omega$). The phase of the current changes rapidly between limiting values of $+\pi/2$ and $-\pi/2$ as we pass through $\pm 30°$ latitude. At the critical latitude current and forcing are in phase so that the transfer of momentum and energy from atmosphere to ocean is significantly increased.

This enhancement of wind stirring by a near-resonant response can be of considerable importance especially in areas of weak tidal currents where there is a well-developed sea breeze regime. In this contribution, we consider a new set of observations from a location close to the resonant latitude in the Southern Hemisphere to investigate the intensity and vertical structure of the current response to diurnal winds.

2. Location and measurement methods

An extended series of measurements, covering the period March 1998 to April 1999, were made by Fugro Geos for Shell Exploration and Production Namibia B.V. at the Kudu field on the Namibian shelf. Here we shall consider the results from a single ADCP mooring deployed at a location (28.6°S, 14.6°E), which is ~133 km from the coast at the outer edge of the shelf in water of depth 175 m (Fig. 2). This location is at the southern end of the Benguela upwelling system. The surface Benguela Current is strongest over the slope (~0.5 m s^{-1})

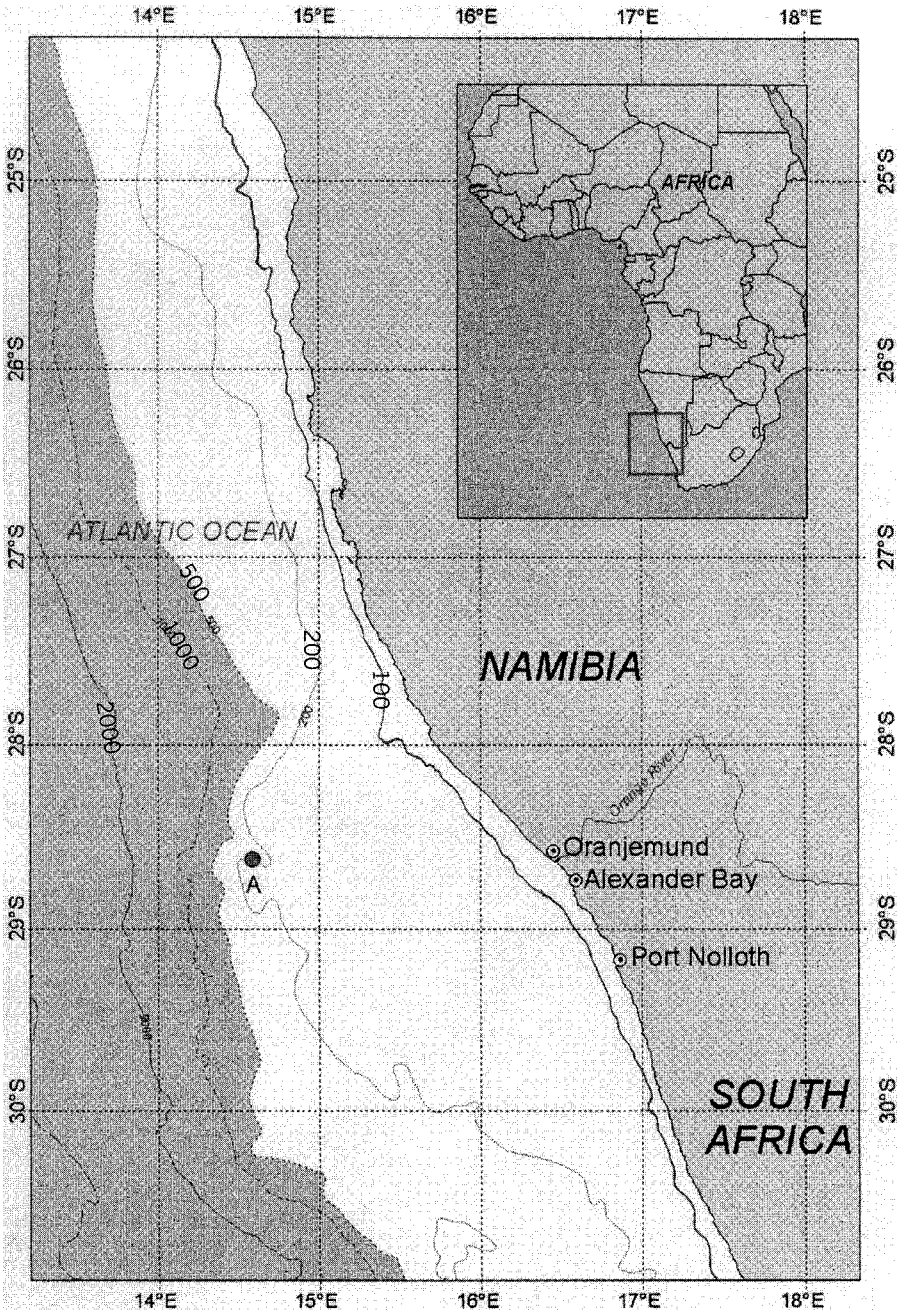

FIG. 2. Location of the observations on the Namibian shelf. The mooring was located at position **A** in water of depth 175 m close to the outer edge of the shelf. Depth contours are shown at 100, 200, 500, 1000, and 2000 m.

but extends onto the shelf where the surface flow is generally to the north with velocities of 0.05–0.20 m s^{-1} (Tomczak and Godfrey 1994). The tides here are predominantly semidiurnal with a range of ~2 m at springs (0.6 m at neaps) but tidal currents are generally small in relation to the wind-driven flow.

At the time of the observations, toward the end of the austral summer, the water column on the shelf was strongly stratified as indicated by the CTD profile (Fig. 3) taken just before deployment of the ADCP mooring. Surface and bottom mixed layers are separated by an interior region of large density gradients. Most of the surface to bottom density difference ($\Delta\sigma_t$ = 2.5 kg m^{-3}) is associated with the temperature difference between the surface (~19.7°C) and the near bed (~10.8°C).

Time series of the current structure were obtained using a pair of ADCP instruments (RDI Workhorse 300

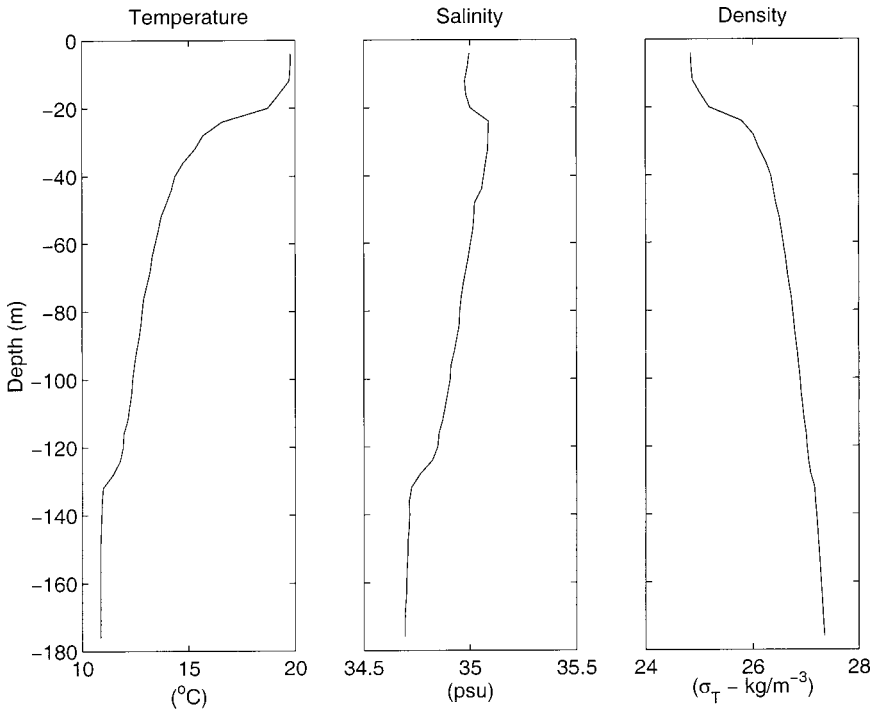

FIG. 3. Temperature, salinity, and density from CTD profile at the mooring location on 9 Mar 1998.

kHz) mounted in midwater on a single mooring. The instruments, one looking upward and the other downward, measured the current profile throughout the water column except for immediate near-surface and near-bed shadow zones (~12 m thick) where sidelobe effects prevent valid measurements. The vertical bin size was set to 8 m and the instruments recorded ensemble means over periods of 10 minutes. A continuous series from both instruments was available for the period 9 March 1998–15 April 1998.

3. The current regime

A general impression of the observed flow over the period of observation is given in Fig. 4, which shows mean flow profiles and the progressive vector diagrams at three depths over the observation period. There is a rather steady northward component of mean flow at all depths (Fig. 4a), which is strongest near the surface (maximum ≈0.11 m s^{-1} at 40 m) and decreasing to ~3 cm s^{-1} at 150 m. The E–W component is generally much weaker with a flow of ~4 cm s^{-1} westward near the surface; changing to a slight eastward flow ≈2 cm s^{-1} between 25 and 125 m.

At all depths there is clear evidence in the progressive vector diagrams (Fig. 4b) of a pronounced anticyclonic component of current rotating once per day. In many cases these diurnal currents exceed the mean flow and cause the flow direction to reverse. This dominance of the circular motions is most apparent during the period 15–23 March when the mean flow was generally weaker. The full structure of the diurnal currents for this period is shown in Fig. 5, which is a synthesis of the data from the upward and downward looking instruments. The data have been subjected to a high-pass filter with a cutoff of 48 h to remove the mean and other low frequency motions while the coordinates have been rotated so that u and v represent cross-slope ($+ve$ to 045°) and alongslope ($+ve$ to 315°) components, respectively.

Presented in this way, the data reveal rather regular current oscillations throughout the water column with almost equal amplitudes for the u and v components. The phase of u leads v by close to $\pi/2$, so the motion is everywhere anticlockwise, but the phase of both components exhibits a pronounced phase shift of $\sim\pi$ radians, centered on 75 m depth and occurring between the upper layer (above 60 m) and the lower layer (below 80 m depth). Motion in the lower layer is only slightly weaker on average than that in the upper layer. The phase of the motion apparently varies rather slowly with depth within the upper and lower layers except near the surface where there are indications of a division of the upper layer associated with the strong pycnocline at ~25 m depth.

Spectral analysis in terms of rotary components (Fig. 6) confirms that, in both upper and lower layers, the currents are entirely dominated by anticlockwise motion in the diurnal-inertial frequency band. A much weaker, semidiurnal, peak indicates tidal motion that is also pre-

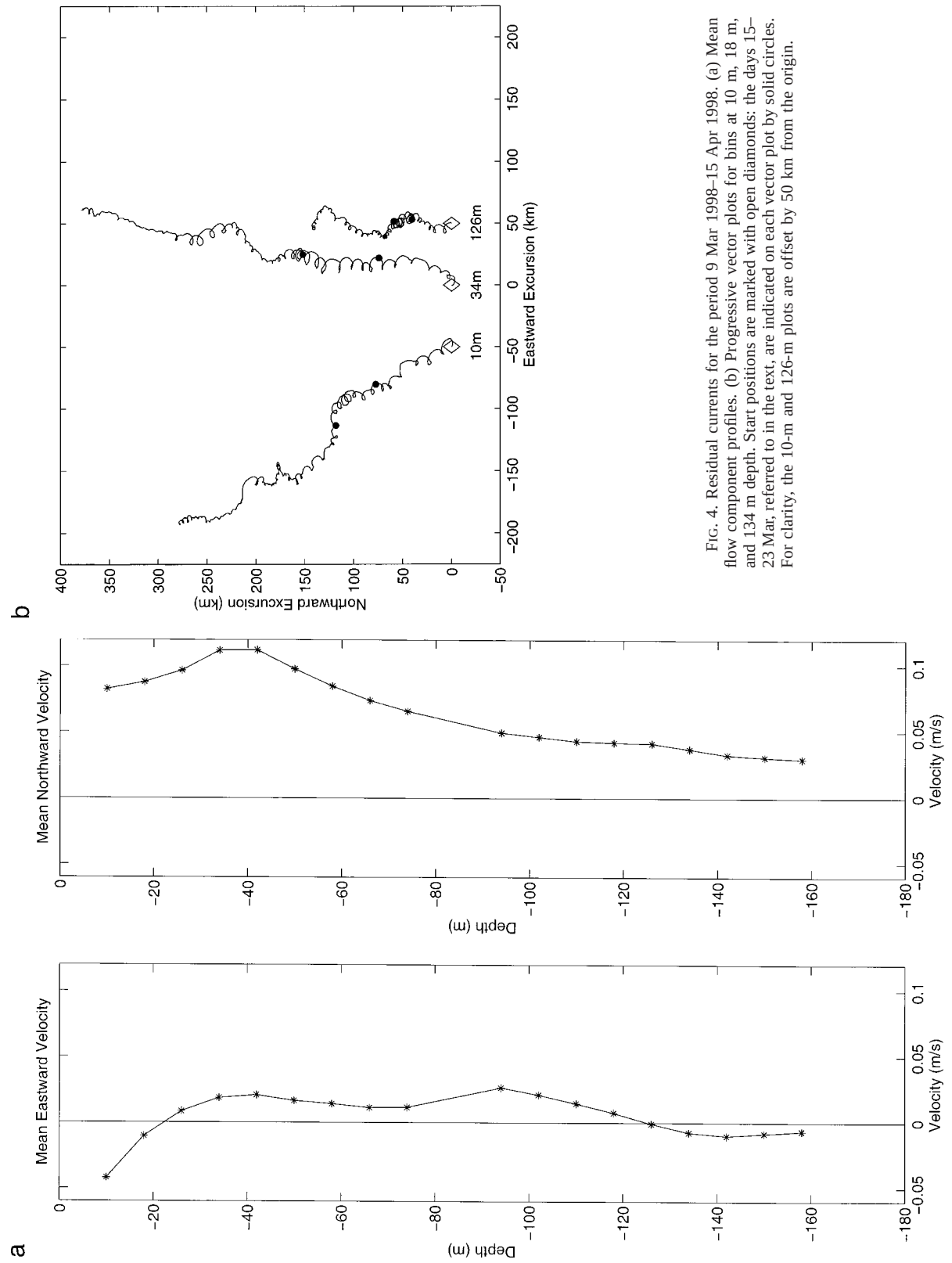

FIG. 4. Residual currents for the period 9 Mar 1998–15 Apr 1998. (a) Mean flow component profiles. (b) Progressive vector plots for bins at 10 m, 18 m, and 134 m depth. Start positions are marked with open diamonds: the days 15–23 Mar, referred to in the text, are indicated on each vector plot by solid circles. For clarity, the 10-m and 126-m plots are offset by 50 km from the origin.

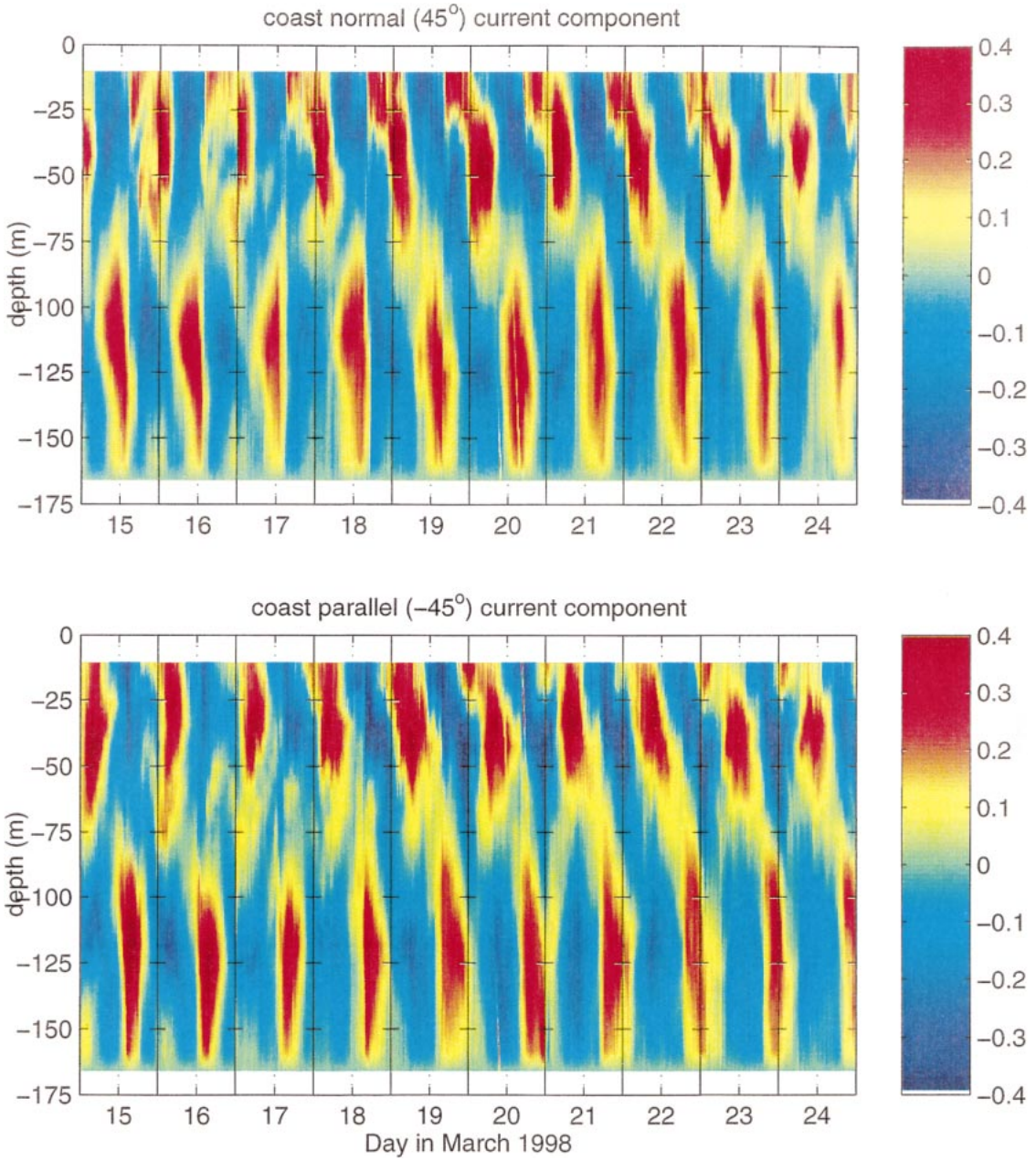

FIG. 5. High frequency currents for 15–24 Mar 1998. Depth–time plots for 10 days of u (coast normal) and v (coast parallel) components in m s^{-1} of high-pass currents (filter cutoff at 48 h) based on the combination of data from the two ADCPs. The water column is covered by measurements at intervals of 8 m except for shadow zones (~12 m thick) near the surface and bottom and at the height of the ADCP instruments where the separation of the closest data bins of the two instruments is ≈20 m.

dominantly anticlockwise in character. Although Fig. 6 shows that energy is present at both diurnal and inertial frequencies, the closeness of the two frequencies at this latitude does not allow us to fully resolve these two components by spectral methods with the available data. We shall, therefore, examine changes in phase of the diurnal oscillation to infer changes between predominantly diurnal and inertial motions.

For each 24-h period we have fitted diurnal rotary components to the full data series to obtain the amplitude and phase of the clockwise and anticlockwise motions (Fig. 7). If the motion was exactly at the diurnal frequency, we would expect the phase to be fixed. At times, the phase is approximately constant (e.g., days 13–15), but generally the phase lag shows a tendency to increase with time at a rate less than, or equal to, the rate of phase lag increase (15.5° d^{-1}) for motion at the local inertial frequency. This pattern

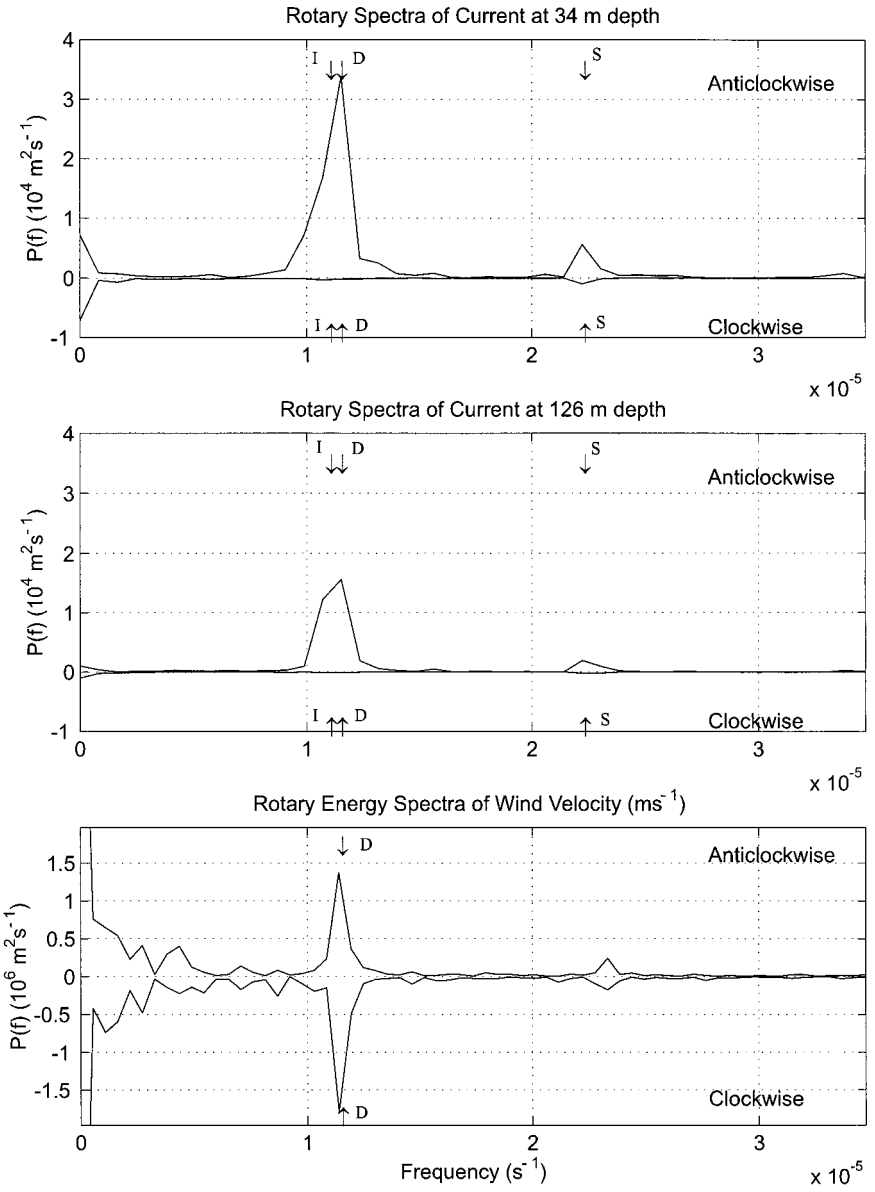

FIG. 6. Rotary energy spectra of currents and wind. Anticlockwise (positive) and clockwise (negative) contributions to kinetic energy density are plotted for (a) currents at 34 m (upper layer), (b) currents at 126 m (lower layer), and (c) wind velocity at Oranjemund airport on the Namibian coast. Arrows indicate inertial (I), diurnal (D) and semidiurnal (S) frequencies

of phase change is consistent with an alternation between periods of forced oscillations when diurnal motion would predominate and periods of decreased forcing when the motion tends to revert to free oscillations at the inertial period.

4. The wind regime

Unfortunately wind data were not recorded at the mooring location. The nearest source of wind data is the airport at Oranjemund, which is close to the Namibian coast but ~150 km from the current meter mooring. Time series from this source provide clear evidence of marked diurnal variations in the wind stress associated with the sea breeze regime, which is a well-known feature of this coast (Hart and Currie 1960). In Fig. 8 the Oranjemund winds are presented as mean and high frequency (>0.5 cycles/day) wind stress components for the period 8–24 March, which covers the time of the current observations in Fig. 5. The mean stress is mostly directed to NE with values up to 0.04 Pa but considerably stronger stresses are associated with the high frequency variations. Cross-shore and alongshore components have maxima of comparable amplitude in mid–

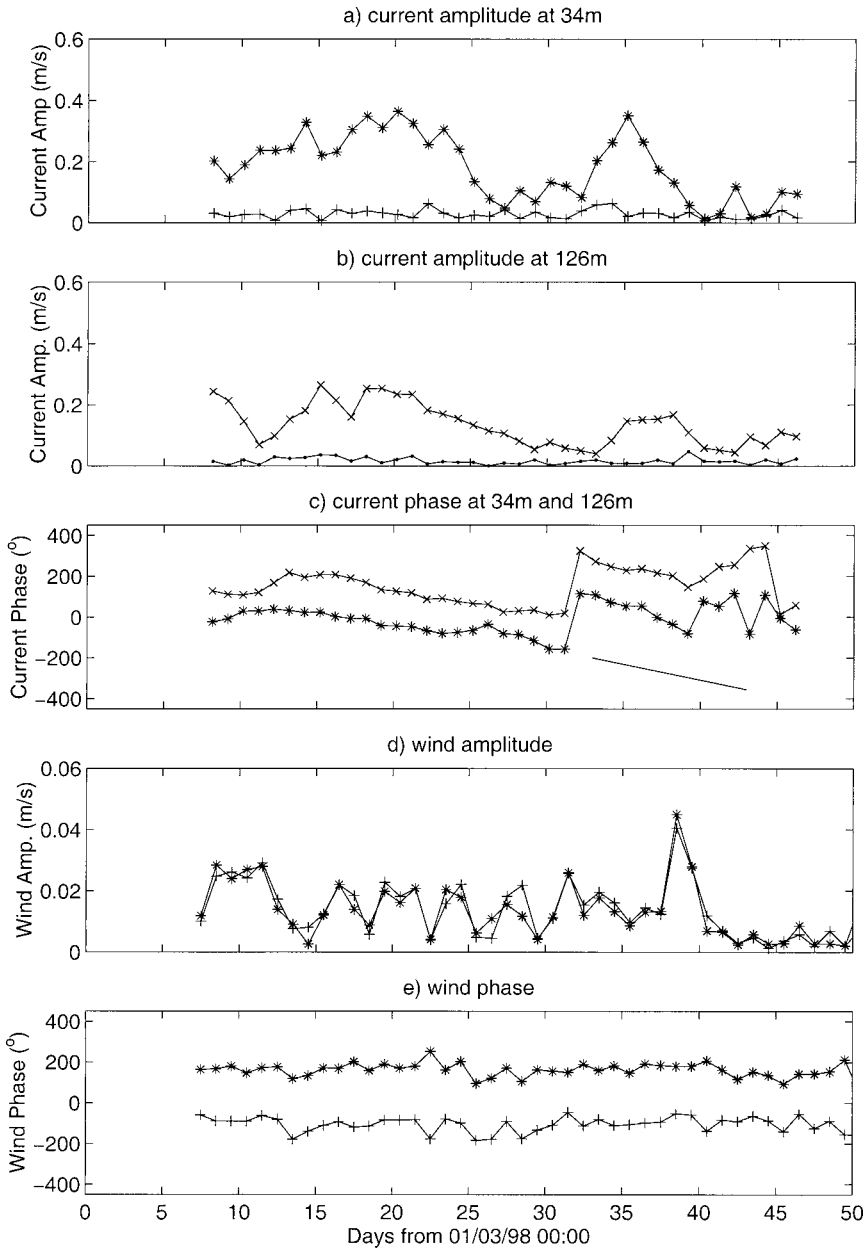

FIG. 7. Amplitude and phase of the diurnal motion over the full recording period. (a) Current at 34-m anticlockwise (*) and clockwise (+), (b) current at 126 m anticlockwise (×) and clockwise (·), (c) phase of anticlockwise component at 34 m (*) and 126 m (×), (d) wind amplitude as anticlockwise (*) and clockwise (+) components, and (e) phase of the wind components (*) anticlockwise and clockwise (+). The straight sloping line in (c) indicates the rate of phase change of a pure inertial oscillation (15.5° h^{-1}).

late afternoon (1500–1800 LT) with peak stresses exceeding 0.1 Pa on some days and much weaker offshore stresses at night. The cross-shore and alongshore diurnal components of the wind vector are almost in phase so the motion is approximately rectilinear at 45° to the coast, that is, N–S, and consists of nearly equal clockwise and anticlockwise components, as can be see in the rotary spectral plots of Fig. 6c.

In a diurnal fit (Fig. 7c), the phase of the rotary components of the wind stress varies little, while the amplitude of the clockwise and anticlockwise components are approximately equal. Over the period of observations, the diurnal wind shows a general, slow decrease although with considerable day-to-day variation. The currents also exhibit a general decrease in energy over the period but there is no clear correlation of currents

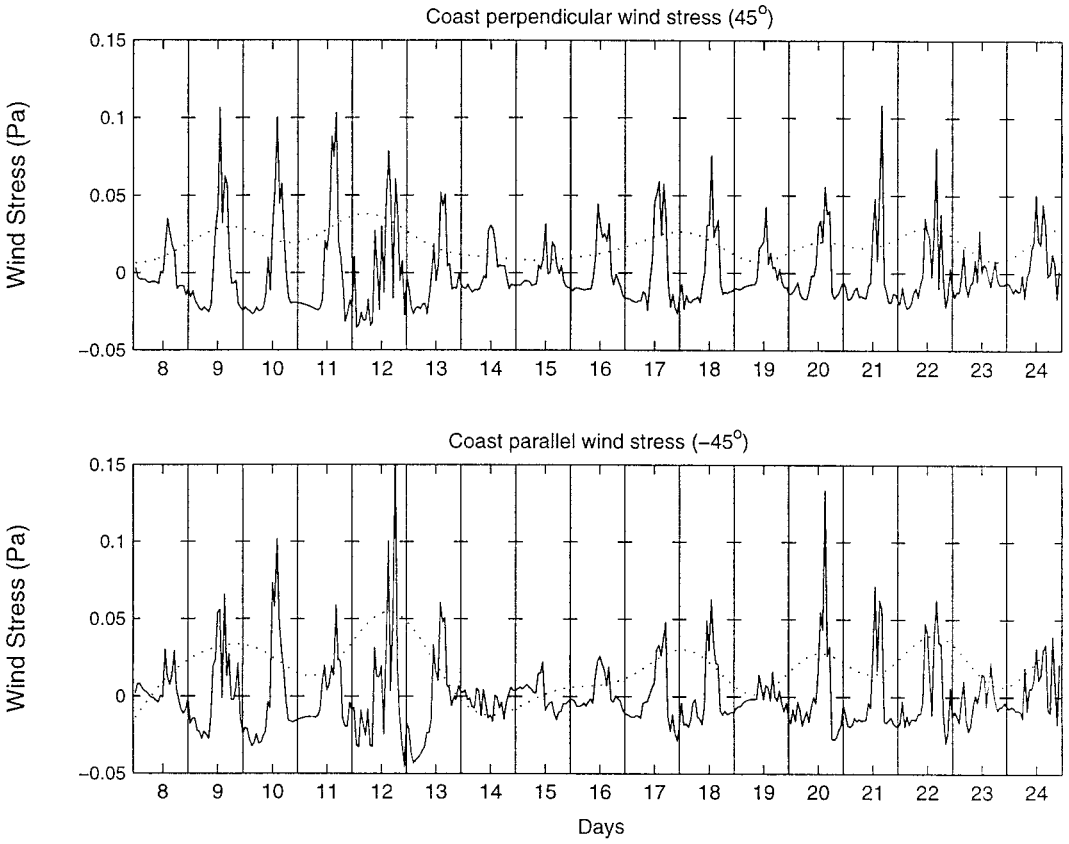

FIG. 8. Time series of the cross-shore and alongshore components of stress (Pa) computed from wind observations at Oranjemund airport for the period 8–24 Mar 1998. The stress has been filtered to show high frequency (continuous line) and low frequency (dotted line) components (filter cutoff at 48 h).

with the wind variations. This is perhaps not surprising in view of the large separation of the sites. Moreover data from a land station may be inappropriate to represent the wind regime over the outer shelf where the diurnal cycle may be influenced by day–night variations in the trade wind regime.

5. Interpretation and model analysis

The picture that emerges from the observations is of a current system in which strong diurnal-inertial oscillations are superimposed on a weaker mean flow to the north. The vertical structure of the diurnal motions consists of two layers oscillating with comparable kinetic energy but ~180 degrees out of phase. This form of vertical structure and the intensity of the current response may be understood in terms of an analytical model to which we now turn.

In the simplest two layer model, we consider flow in a shelf region bounded by a coastline extending in the y direction at $x = 0$ and with a depth profile $H(x)$. The layers are assumed to be uniform in density and velocity but decoupled from each other by a frictionless interface, while the motion is forced by an oscillatory wind stress (τ_x, τ_y) at the diurnal frequency ω. The momentum equations may be written for the upper and lower layers, respectively, as

$$\frac{\partial u_1}{\partial t} - fv_1 = \frac{\tau_x}{\rho h_1} - g\frac{\partial \eta}{\partial x}; \qquad \frac{\partial v_1}{\partial t} + fu_1 = \frac{\tau_y}{\rho h_1}, \quad (3)$$

$$\frac{\partial u_2}{\partial t} - fv_2 = -g\frac{\partial \eta}{\partial x}; \qquad \frac{\partial v_2}{\partial t} + fu_2 = 0, \quad (4)$$

where η is the surface elevation. Providing that the shelf width L is small in relation to the barotropic wavelength $2\pi(gH)^{1/2}/\omega$, we may employ the lowest order vertically integrated solution (Craig 1989b) in order to determine the surface slope as

$$\frac{\partial \eta}{\partial x} = \frac{\tau_x + i(f/\omega)\tau_y}{\rho g H}. \quad (5)$$

Because of the no-normal-flow condition at the coast, the diurnal cross-slope stress τ_x induces an opposing surface slope. Similarly the alongshore wind stress τ_y drives a

coast-parallel, depth uniform current $V = i\tau_y/(\omega gH)$ that, in geostrophic balance, requires a surface slope component of amplitude $(f/\omega)\tau_y/(\rho gH)$. Unlike the wind stress, which acts directly only at the surface, the pressure gradient associated with the surface slope operates throughout the water column. Substituting Eq. (5) into (3) and (4) and defining the complex velocity $w = u + iv = We^{i\omega t}$, the governing equations for the complex amplitudes W_1 and W_2 become

$$i(\omega + f)W_1 = \frac{T_x + iT_y}{\rho h_1} - \left(T_x + \frac{if}{\omega}T_y\right)\Big/\rho H$$

$$i(\omega + f)W_2 = -\left(T_x + \frac{if}{\omega}T_y\right)\Big/\rho H, \qquad (6)$$

where T_x and T_y represent the amplitudes of the stress components and we have replaced the time derivatives with $i\omega$; positive ω corresponds to anticlockwise motion.

Rearranging and putting $\gamma = h_2/h_1$, we have the regular oscillatory solutions for anticlockwise motion:

$$W_1 = \frac{\gamma T_x + i(\gamma + f/\omega + 1)T_y}{i\rho H(f + \omega)};$$

$$W_2 = \frac{-(T_x - if/\omega T_y)}{i\rho H(f + \omega)}. \qquad (7)$$

Close to the resonant latitude in the Southern Hemisphere $f/\omega \to -1$ so that

$$W_1 \approx \frac{\gamma(T_x + iT_y)}{\rho H(f + \omega)} \approx -\gamma W_2, \qquad (8)$$

which indicates that the phase of the motion will differ by 180 degrees between the two layers and that the ratio of the velocity amplitude in the two layers will be γ, which is of order unity in the present case so that upper and lower layer motions will be of comparable magnitude. While the anticlockwise response will be enhanced at latitudes close to 30°S where $f = -\omega$, the response to cyclonic forcing ($\omega = f$) at the diurnal frequency is considerably weaker by a factor of $|(f + \omega)|/|(f - \omega)|$. This ratio has a value of ≈47 for latitude 28.6°S so that, for equal forcing, anticlockwise motions should be minimal as observed.

This model explains the key features of the observations, namely, the enhanced anticyclonic current response, the energetic motions in the lower part of the water column, and the 180 degree phase shift between upper and lower layers. The observed phase change is centered on a depth of 75 m, which would imply a value of $\gamma = 1.33$, a value comparable with the ratio of maximum current amplitudes in the upper and lower layers for the data of Fig. 5.

6. Summary and discussion

At this outer shelf location, close to the critical latitude, the current regime in a period during late austral summer was found to be dominated by oscillatory flows in the diurnal-inertial band. The motions in this band are almost pure anticlockwise circular currents with speeds up to 40 cm s^{-1} and a kinetic energy content, which is an order of magnitude bigger than that associated with the mean flow, which is to the north at a speed ≈10 cm s^{-1}. Energetic anticlockwise currents extend throughout the water column with lower layers oscillating in antiphase to the near-surface motion.

We interpret the observed behavior of the oscillatory currents in terms of wind-forced flow. The essential component in our model is the Craig condition [Eq. (5)], which defines the crucial role of the coastal boundary in inducing a pressure gradient in response to surface stress forcing. This pressure gradient effectively transfers the wind forcing to the whole water column with a phase shift of ~180 degrees that is reflected in the current response. Momentum is thus able to enter the lower layer without having to be transferred downward through the shear stress as in classical Ekman theory. Our analytical model completely omits the latter mechanism but still gives a plausible account of the observations. In order to apply the Craig condition, which derives from the lowest order vertically integrated solution, there is a requirement that the ratio of the shelf width L to the barotropic wavelength $2\pi(gH)^{1/2}/\omega$ should be small. In the present case, where $L \approx 150$ km and the average depth $H \approx 100$ m, the ratio is ~0.055 so that this approximation is appropriate.

We have tested our interpretation further using a 1D numerical version of our model that employs the same basic dynamics as the analytical model but allows us to include the effects of frictional coupling between layers. This numerical model confirms the key role of the Craig condition in determining the vertical structure of amplitude and phase of the flow and shows that, for the range of parameters relevant to the Namibian shelf, the addition of internal shear stresses does not greatly modify the frictionless response to regular forcing. The numerical model has also enabled us to investigate the interaction between the forced diurnal and transient solutions and to demonstrate that, when forcing is interrupted, the motion switches to the inertial frequency so that, when viewed as a diurnal motion, there is a regular increase in the phase lag with time as observed (Fig. 7). The combination of diurnal and inertial oscillations creates a beat cycle that, at latitudes farther from 30°, may be a prominent feature of the velocity field (Rippeth et al. 2001).

We propose that the basic mechanism involved in our model is responsible for the form of vertical structure reported for other cases of diurnal-inertial oscillations at locations that may be influenced by land boundaries (Chen et al. 1996; DiMarco et al. 2000; Rippeth et al. 2001). The observed phase change between upper and lower layers is, in our view, not primarily due to phase propagation effects such as occur for inertial waves, but results from the direct transfer of forcing to the lower

layers by the induced pressure gradient that is in antiphase with the near-surface forcing. This phase change was simulated in a numerical model of the response of the Texas–Louisiana shelf by Chen and Xie (1997), who point to the role of the no flux condition at the coastal boundary in inducing reverse flow in the bottom layer.

The occurrence of strong diurnal oscillations on the outer Namibian shelf reported here, and also in the recent surface drifter observations of Largier and Boyd (2001), implies the existence of substantial diurnal forcing at shelf edge. This may seem surprising in view of the distance from coast and that sea breeze systems are generally thought not to extend much more than ~100 km from the coast (Simpson 1994). Halpern (1977), however, reports significant diurnal winds extending to an offshore site ~125 km from the coast of north Africa at latitude 22°N.

The near-resonant response observed in this case involves an efficient transfer of momentum and energy from the wind field to the current system with the diurnal motions dominating the kinetic energy spectrum. The antiphase motions in top and bottom layers involve substantial vertical shears, which will tend to promote dissipation and vertical mixing through the water column. In shelf areas with significant diurnal winds and located close ($\pm 10°$) to the critical latitude, this energy source may be an important mechanism for inducing mixing between upper and lower layers. Where, as in the case considered here, tidal forcing is weak, motions in the diurnal-inertial band may be the dominant mechanism for vertical exchange through a stratified water column.

Acknowledgments. We would like to acknowledge the generosity of Shell Exploration and Production Namibia B. V. in making this valuable dataset available to us for scientific research. We would also like to thank Fugro Geos Ltd. and in particular Jon Upton for providing the data and assisting throughout the project.

REFERENCES

Battisti, D. S., and A. J. Clarke, 1982: A simple method for estimating barotropic currents on continental margins with specific reference to the M_2 tide on the Atlantic and Pacific coasts of the United States. *J. Phys. Oceanogr.*, **12,** 8–16.

Chen, C., and L. Xie, 1997: A numerical study of wind-induced, near-inertial oscillations over the Texas–Louisiana shelf. *J. Geophys. Res.,* **102,** 15 583–15 593.

——, R. O. Reid, and W. D. Nowlin, 1996: Near-inertial oscillations over the Texas–Louisiana shelf. *J. Geophys. Res.,* **101,** 3509–3524.

Craig, P. D., 1989a: Constant eddy-viscosity models of vertical structure forced by periodic winds. *Cont. Shelf Res.,* **9,** 343–358.

——, 1989b: A model of diurnally forced vertical current structure near 30° latitude. *Cont. Shelf Res.,* **9,** 965–980.

DiMarco, S. F., M. K. Howard, and R. O. Reid, 2000: Seasonal variation of wind-driven diurnal current on the Texas–Louisiana shelf. *Geophys. Res. Lett.,* **27,** 1017–1020.

Gustafson, T., and B. Kullenberg, 1933: Tragheitsstromungen in der Ostsee. *Medd. Gotesborg Oceanogr. Inst.,* **5**.

Halpern, D., 1977: Description of the wind and of upper ocean current and temperature variations on the continental shelf of northwest Africa during March and April 1974. *J. Phys. Oceanogr.,* **7,** 422–430.

Hart, T. J., and R. I. Currie, 1960: The Beneguela Current. *Discovery Rep.,* **31,** 123–298

Helland-Hansen, B., and V. W. Ekman, 1931: Measurements of ocean currents (Experiments in the North Atlantic). *Kgl. Fysiiogr. Sallsk. Lund,* **1**.

Largier, J., and A. Boyd, 2001: Drifter observations of surface water transport in the Benguela Current during winter 1999. *South Afr. J. Sci.,* **97,** in press.

Millot, C., and M. Crépon, 1981: Inertial oscillations on the continental shelf of the Gulf of Lions—observations and theory. *J. Phys. Oceanogr.,* **11,** 639–657.

Pattiaratchi, C., B. Hegge, J. Gould, and I. Eliot, 1997: Impact of sea-breeze activity on nearshore and foreshore processes in southwestern Australia. *Cont. Shelf Res.,* **17,** 1539–1560.

Pollard, R. T., 1980: Properties of near-surface inertial oscillations. *J. Phys. Oceanogr.,* **10,** 385–397.

——, and R. C. Millard, 1970: Comparison between observed and simulated wind-generated inertial oscillations. *Deep-Sea Res.,* **17,** 813–821.

——, P. B. Rhines, and R. O. R. Y. Thompson, 1973: The deepening of the wind-mixed layer. *Geophys. Fluid Dyn.,* **3,** 381–404.

Poulain, P. M., 1990: Near-inertial and diurnal motions in the trajectoreis of mixed layer drifters. *J. Mar. Res.,* **48,** 793–823.

Rippeth, T. P., J. H. Simpson, R. J. Player, and M. Garcia, 2001: Current oscillations in the diurnal-inertial band on the Catalonian Shelf in spring. *Cont. Shelf Res.,* in press.

Rosenfeld, L. K., 1988: Diurnal period wind stress and current fluctuations over the continental shelf off northern California. *J. Geophys. Res.,* **93** (C3), 2257–2276.

Salat, J., J. Tintore, J. Font, D. P. Wang, and M. Vieira, 1992: Near-inertial motion on the shelf–slope front off northeast Spain. *J. Geophys. Res.,* **97** (C5), 7277–7281.

Schahinger, R. B., 1988: Near-inertial motions on the South Australian shelf. *J. Phys. Oceanogr.,* **18,** 492–504.

Simpson, J. E., 1994: *Sea Breeze and Local Wind.* Cambridge University Press, 234 pp.

Tomczak, M., and J. S. Godfrey, 1994: *Regional Oceanography: An Introduction.* Pergamon, 422 pp.

Webster, F., 1968: Observations of inertial period motions in the deep-sea. *Rev. Geophys.,* **6,** 473–490.

Webster, I., 1986: The vertical structure of currents on the north-west shelf of Australia at subtidal frequencies. *J. Phys. Oceanogr.,* **16,** 1145–1157.